ghg GREENHOUSE GASES SCIENCE AND TECHNOLOGY

Transient CO_2 leakage and injection in wellbore-reservoir systems for geologic carbon sequestration†

Lehua Pan, Curtis M. Oldenburg, and Karsten Pruess, Lawrence Berkeley National Laboratory, University of California, Berkeley, CA, USA
Yu-Shu Wu, Colorado School of Mines, Golden, CO, USA

Abstract: At its most basic level, the injection of CO_2 into deep reservoirs for geologic carbon sequestration (GCS) involves a system comprising the wellbore and the target reservoir, the wellbore being the only conduit available to emplace the CO_2. Wellbores in general have also been identified as the most likely conduit for CO_2 and brine leakage from GCS sites, especially those in sedimentary basins with historical hydrocarbon production. We have developed a coupled wellbore and reservoir model for simulating the dynamics of CO_2 injection and leakage through wellbores, and we have applied the model to situations relevant to geologic CO_2 storage involving upward flow (e.g. leakage) and downward flow (injection). The new simulator integrates a wellbore-reservoir system by assigning the wellbore and reservoir to two different sub-domains in which flow is controlled by appropriate laws of physics. In the reservoir, we model flow using a standard multiphase Darcy flow approach. In the wellbores, we use the drift-flux model and related conservation equations for describing transient two-phase non-isothermal wellbore flow of CO_2-water mixtures. Applications to leakage test problems reveal transient flows that develop into quasi-steady states within a day if the reservoir can maintain constant conditions at the wellbore. Otherwise, the leakage dynamics could be much more complicated than the simple quasi-steady-state flow, especially when one of the phases flowing in from the reservoir is near its residual saturation. A test problem of injection into a depleted (low-pressure) gas reservoir shows transient behavior out to several hundred days with sub-critical conditions in the well disappearing after 240 days.

Key words: CO_2 injection; CO_2 leakage; numerical modeling; wellbore reservoir

Introduction

As discrete pathways through geologic formations, boreholes and wells are critical to the success of geologic carbon sequestration (GCS) projects because of the access they provide to storage reservoirs for site characterization, CO_2 injection, monitoring, and fluid withdrawal. On the other hand, boreholes and wells – in particular, deep abandoned wells from oil or gas exploration and production

Correspondence to: Lehua Pan, Earth Sciences Division, Lawrence Berkeley National Laboratory, University of California, Berkeley, CA 94720, USA. E-mail: lpan@lbl.gov

Received June 24, 2011; revised August 26, 2011; accepted August 30, 2011
Published online at Wiley Online Library (wileyonlinelibrary.com). DOI: 10.1002/ghg.41

activities – are also potential leakage pathways for injected CO_2 and displaced brine. Critical to the efficient and safe implementation of GCS is a detailed understanding of flow and transport processes in boreholes to control CO_2 injection and to model potential leakage up the borehole. In order to facilitate an understanding of borehole-flow and transport processes coupled with target reservoirs, and to improve the design of injection operations, we have developed a borehole-reservoir flow simulator for CO_2 and variable salinity water that models transient non-isothermal processes in deep boreholes and reservoirs including multiphase flow with CO_2 transitions from supercritical to gaseous conditions. In this paper, we present two example problems of wellbore-reservoir coupling for leakage and injection that show the capabilities of the new simulator along with demonstrating some of the significant transient multiphase flow phenomena that can occur in flowing wells. Although the modeling capability we have developed could be used to model flow up open annular regions of the well – for example, outside of the main well casing – all of the examples shown here are for flows within the open circular cross-sectional part of the well.

Background and motivation

Wellbores are the critical element of GCS systems insofar as leakage and injection are concerned. On the leakage side, wellbores are widely recognized as the main possible leakage pathway capable of conveying CO_2 or brine to groundwater resources leading to potential groundwater contamination[1–3] as well as impacting storage effectiveness should leakage occur.[4,5] In addition to their role in potential leakage, wellbores are the main injection system element and there are concerns about controlling CO_2 phase conditions in the well. This concern arises because of the particular sensitivity of phase stability of CO_2 around commonly encountered pressures and temperatures in typical GCS wells. In particular, low pressure reservoirs or very high permeability reservoirs may allow two-phase conditions to develop in the well during injection of CO_2 in its liquid or supercritical forms with resulting decrease in mass flow rate.[6,7] Addressing quantitatively both leakage and injection aspects of wellbore flow processes in GCS systems requires the ability to model coupled wellbore-reservoir processes.

Prior work in quantitative modeling of CO_2 leakage and injection processes includes the model developed by Lu and Connell[8] which was a quasi-steady numerical approach that included two-phase flow of CO_2 and used a productivity index approach to couple the wellbore to the reservoir. More recently, Lindeberg[7] included transient effects of two-phase CO_2 flows in the well without coupling to the reservoir. Remoroza *et al.* [9] developed an approach for geothermal applications that coupled the wellbore flow with the reservoir but assumed steady-state and single-phase flow in the well. Although there exist fully coupled wellbore-reservoir flow simulators for oil/gas industry applications,[10] a transient, multiphase and multicomponent wellbore simulator with full coupling to the reservoir applicable to CO_2-brine flows for GCS has not been previously developed to our knowledge. To fill the need to address important wellbore leakage and injection problems, we have developed a coupled wellbore-reservoir modeling capability for the highly non-isothermal, two-phase and multicomponent flows that may arise in CO_2-brine leakage and CO_2 injection processes.

Overview of method

The new wellbore flow model is based on the drift-flux model (DFM) approach[11,12] and extends TOUGH2/ECO2N[13, 14] to be applicable for wellbore flow coupled to reservoir flow. Unlike the coupling approach used in earlier efforts, the deliverability option in TOUGH2[15] is not used and the flow inside the wellbore is not assumed to be at steady state. The 'equivalent Darcy media' approach for the mixture velocity[16] is not used either Instead, the new model (T2Well/ECO2N) uses an integrated wellbore-reservoir system of CO_2-brine in which the wellbore and reservoir are two different sub-domains where flow is controlled by different physics, specifically viscous flow in the wellbore governed by the one-dimensional drift-flux model (DFM), and three-dimensional flow through porous media in the reservoir is governed by a multiphase version of Darcy's Law. The detailed description, mathematical formulation, and verification of T2Well/ECO2N are presented in the T2Well/ECO2N User's Guide[17] and in the proceedings of an earlier conference.[18] For completeness, we briefly summarize the DFM as implemented in T2Well/ECO2N.

In the following discussion and thereafter, the term 'gas' or 'gas phase' refers to the CO_2-rich phase

  | *Greenhouse Gas Sci Technol.* **1**:335–350 (2011); DOI: 10.1002/ghg

whereas the term 'liquid' or 'liquid phase' refers to the water-rich phase (or brine). In other words, CO_2 in gas phase (i.e. the CO_2-rich phase) could be formally gaseous, liquid, or, supercritical CO_2 depending on the local *P-T* conditions. However, by this terminology CO_2 in the liquid phase is CO_2 dissolved in water or brine. While not ideal, this terminology is compatible with the existing two-phase DFM terminology which requires a gas and liquid with liquid denser than gas, and it is acceptable for GCS systems where formal liquid CO_2 conditions (i.e. conditions on the CO_2 phase diagram where pressures are higher than those along the liquid-gas phase boundary and $T < 31$ °C) are rare due to the geothermal gradient and relatively great depths of GCS systems.

Directly solving the momentum equations of two-phase flow is difficult and often not practical because the wellbore equations need to be coupled to a reservoir simulator. The DFMs, first developed by Zuber and Findlay[12] and Wallis,[19] among others, provide a simpler way to tackle the problem. Although various nomenclatures and forms of equations were used to describe the DFM in the literature over decades, the basic idea of the DMFs is to assume that the gas velocity, u_G, can be related to the volumetric flux of the mixture, *j*, and the drift velocity of gas, u_d, by the empirical constitutive relationship in Eqn (1):

$$u_G = C_0 j + u_d \tag{1}$$

where C_0 is the profile parameter to account for the effect of local gas saturation and velocity profiles over the pipe cross-section. The liquid velocity u_L can be solved by considering the definition of the volumetric flux of the mixture as

$$u_L = \frac{1 - S_G C_0}{1 - S_G} j - \frac{S_G}{1 - S_G} u_d \tag{2}$$

where S_G is the gas phase saturation.

With the DMF (1) – (2), the momentum equations of two-phase flow in a wellbore can be simplified into a single equation in terms of the mixture velocity u_m and the drift velocity u_d as follows:

$$\frac{\partial}{\partial t}(\rho_m u_m) + \frac{1}{A}\frac{\partial}{\partial z}\left[A\left(\rho_m u_m^2 + \gamma\right)\right] = -\frac{\partial P}{\partial z} - \frac{\Gamma f \rho_m |u_m| u_m}{2A} - \rho_m g \cos\theta \tag{3}$$

where the term $\gamma = \frac{S_G}{1 - S_G}\frac{\rho_G \rho_L \rho_m}{\rho_m^{*2}}[\{C_0 - 1\}u_m + u_d]^2$ is caused by slip between the two phases. ρ_m, u_m, and ρ_m^* are the mixture density, the mixture velocity (mass center), and the profile-adjusted average density of the mixture.

Therefore, with the DFM approach, solving the complicated momentum equations of two-phase flow becomes an easier task with two steps. First, we obtain the mixture velocity by solving the momentum Eqn (3) and the drift velocity from empirical relationships. Second, we calculate the gas velocity and the liquid velocity as a function of u_m and u_d.

The empirical relationships for the drift velocity and the profile parameter used in T2Well/ECO2N are based on the DFM developed by Shi *et al.*[11] They proposed functional forms for the profile parameter and drift velocity with a set of optimized parameters obtained from an extensive set of large-scale pipe flow experiments performed by Oddie *et al.*[20] for one-, two-, and three-phase flows at various inclinations, that can be applied continuously for all flow regimes from bubble flow to film flow. The following is a summary of the mathematical formulations related to the drift velocity proposed by Shi *et al.*[11] that are implemented in T2Well.

First, the drift velocity is calculated as a function of gas saturation and other fluid properties:

$$u_d = \frac{(1 - C_0 S_G)\, u_c K(S_G, K_u, C_0,)\, m(\theta)}{C_0 S_G \sqrt{\rho_G/\rho_L} + 1 - C_0 S_G} \tag{4}$$

where $m(\theta)$ describes the inclination (of the wellbore) effect, K_u is the Kutateladze number, a function of Bond number, N_B (i.e., square of dimensionless wellbore diameter).[21] The 'characteristic velocity', u_c, is a measure of the velocity of bubble rise in a liquid column, a function of fluid properties including the surface tension. The function $K(\bullet)$ in (4) is used to make a smooth transition of drift velocity between the bubble-rise stage and the film-flooding stage.

Second, the profile parameter C_0 is calculated using the same formulas suggested by Shi *et al.*[11] as listed below (with different symbols) for completeness:

$$C_0 = \frac{C_{\max}}{1 + (C_{\max} - 1)\eta^2} \tag{5}$$

where η is a parameter reflecting the effects of the flow status on the profile parameter, a function of gas saturation and the relative mixture velocity. $C_{\max}$ is the user specified maximum profile parameter (usually between 1.0 and 1.5). Detailed discussions and justifications about the formulas (4 – 5) can be found in Shi *et al.*[11] and the implementation details of the drift flux model can be found in Pan *et al.*[17] A verification against an analytical solution of two-phase flow is presented in Appendix A.

In addition to the process modeling capabilities inherited from TOUGH2[22] and TOUGH2/ECO2N,[14] T2Well/ECO2N also describes the following flow processes: (i) upward or downward wellbore flow of CO_2 and variably saline water with transition from supercritical to gaseous CO_2 including Joule-Thomson cooling, (i) exsolution of CO_2 from the aqueous phase as pressure drops, (iii) cross flow into or interaction with layers of surrounding rock (formations), and (iv) two-phase, non-isothermal wellbore flow including countercurrent flow (e.g. gas up and liquid down). Note that, similar to TOUGH2/ECO2N, the model can describe single- and two-phase flows of CO_2-water-NaCl mixtures, but cannot in its current form describe three-phase conditions such as would arise for CO_2-brine mixtures for $T < 31$ °C and with pressures along the CO_2 gas-liquid phase boundary.[23]

Applications to geologic carbon sequestration

Case 1. CO_2 leakage up a wellbore from an infinite reservoir

This problem is an idealized case of non-isothermal two-phase flow up an open wellbore initially filled with water. The scenario envisioned is the tip of a migrating (supercritical) CO_2 plume at 10% gas (CO_2-rich phase) saturation encountering an open well initially filled with water. The focus here is on flow in the wellbore. The reservoir is assumed to be able to maintain constant pressure, temperature, and gas saturation (same as those in reservoir) during the process appropriate for the case of a very large reservoir with high transmissivity. Starting from hydrostatic conditions and a geothermal temperature gradient in the well, an overpressure of 0.1 MPa (1 bar) is applied to the reservoir (represented as the boundary conditions at the well bottom) to mimic an injection-induced overpressure. Wellbore heat transmission to the formation is calculated with the analytical solution of Ramey.[24] A 1D grid of 102 grid cells was used. The major parameters used in the simulation are shown in Table 1.

Table 1. Parameters for Case 1, two-phase CO_2 flow through a wellbore.

Parameter	Value	Note
Length	1,000 m	Vertical wellbore
Diameter	0.1 m	Circular
Thermal conductivity	2.51 W/m °C	used in calculation of lateral heat exchange between the wellbore and the surrounding formation
Boundary conditions at well bottom	P = 9.984 MPa *T* = 65 °C Gas saturation = 10%	Assumed to be constant
Boundary conditions at wellhead	P = 0.1035 MPa *T* = 35 °C	High *T* to avoid coexisting of gaseous and liquid (*T* < 31 °C) CO_2 Gas saturation at wellhead boundary is not fixed (leakage condition)
Initial conditions in wellbore	Hydraulic-static pressure distribution Linear distribution of temperature from 35 °C (wellhead) to 65 °C (well bottom)	
Brine salinity (NaCl)	0.0 (no-salt case) or 0.012 (kg/kg)	Unit: mass fraction of salt in liquid phase

Results as shown in Fig. 1 reveal that early-time upward flow of water within the well at all depths is driven by the 0.1 MPa pressure perturbation at the bottom. Significant gas (CO_2-rich phase) flow begins at approximately $t = 10$ s when a free gas phase evolves at the bottom. By $t \approx 200$ s, gas flows at the middle and top of the well. The sharp peak of water flow rate through the top at about 200 s is related to the breakthrough of the gas phase (a sudden loss of water cap). The passage (breakthrough) of CO_2-rich phase through the upper portion of the wellbore takes place in a very short time period as evidenced by the very short time delay between the gas flow rates at top and middle, a feature of the gas-lift effect, whereby the presence of lower-density gas in the wellbore allows the reservoir pressure to accelerate upward flow in the wellbore. The flow rate of CO_2 reaches approximately 2.33 kg/s in this open wellbore case. The gas phase

  | *Greenhouse Gas Sci Technol.* **1**:335–350 (2011); DOI: 10.1002/ghg

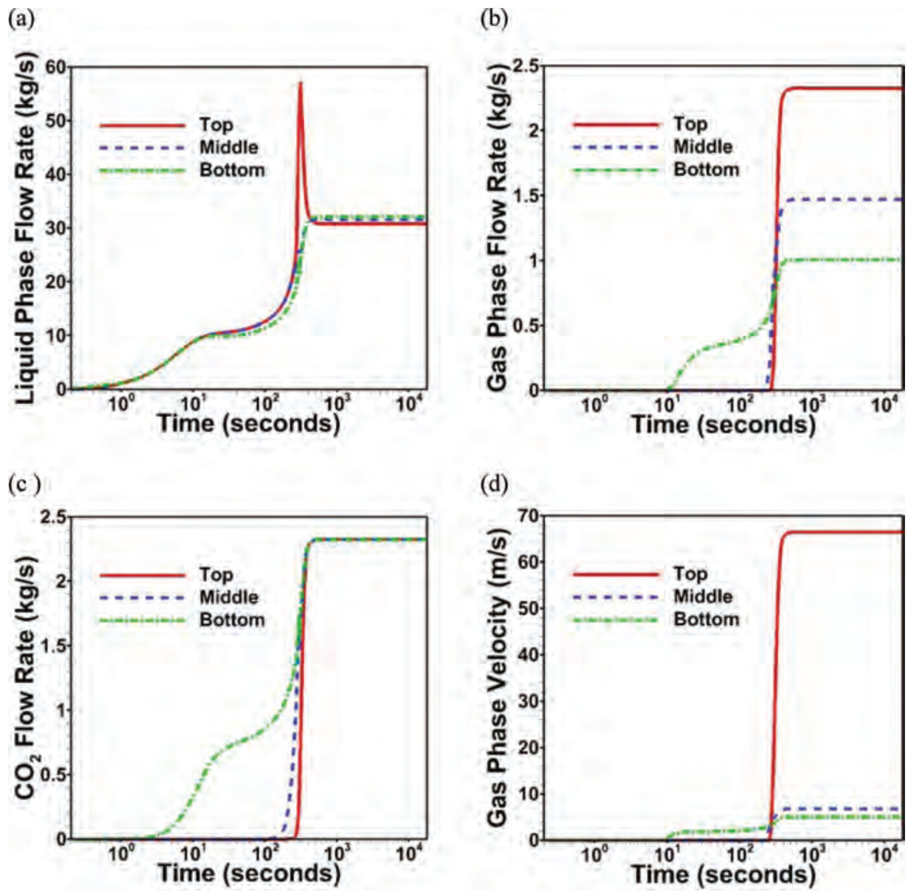

Figure 1. Case 1: Flow rates and velocities of liquid (H_2O-rich phase), gas (CO_2-rich phase), and CO_2 (component) at three levels in the well (bottom, middle, and top).

velocity at the top is much higher than at the middle and bottom, reflecting the acceleration of the gas (CO_2-rich) phase flow when it transitions from supercritical to gaseous conditions.

Further insight into the processes modeled can be obtained from Fig. 2, which shows gas saturation, gas density, pressure, and temperature throughout the well as a function of time. As shown in Fig. 2, the wellbore is initially filled with water and gas enters progressively from the bottom up. After 10 min (600 s), gas distribution is fairly stable in the well from 10% at the bottom to nearly all gas at the top. The reason for this increase in gas saturation is the exsolution of gas from the aqueous phase as fluid pressures decline up the wellbore, amplified by the large expansion that CO_2 undergoes as it transitions from supercritical to gaseous conditions. This transition occurs around the critical pressure (7.4 MPa or 74 bar) at a depth of approximately 755 m. The gas density plot of Fig. 2 shows the sharper decrease in gas density in that region than the region above, although the decrease is less sharp than it would be if the temperature were below the critical temperature of 31 °C (i.e. crossing the CO_2 liquid-gas phase boundary). Temperature also affects CO_2 solubility, but temperature becomes relatively constant as the steady flow develops, resulting in decreasing CO_2 mass fractions being controlled mostly by pressure. The temperature contours show the evolution from a conductive profile controlled by the geothermal gradient to an advective profile controlled by upward fluid flow. At intermediate times between the initial highly transient and the late-time quasi-steady states, there are some local maxima arising from the expansion of CO_2 as warmer fluid rises upwards and transitions to gaseous conditions.

Figure 3(a) shows the CO_2 leakage rates at the wellhead from a fresh-water aquifer and an NaCl-brine aquifer under the same conditions. The final

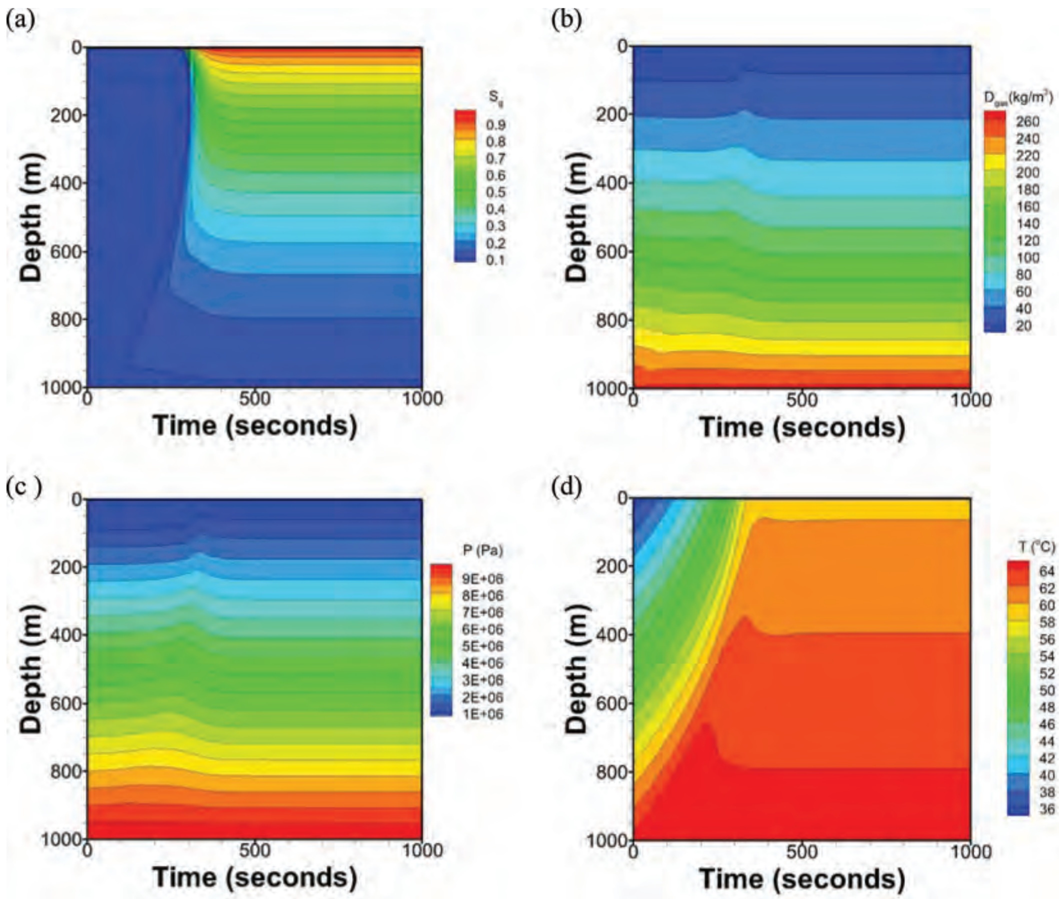

Figure 2. Case 1: Profiles of (a) gas saturation, (b) gas density, (c) pressure, and (d) temperature in the wellbore as a function of time.

flow rate is reduced from 2.33 kg/s for the no-salt case to 1.63 kg/s for brine, accompanied by a slight delay in the breakthrough of CO_2. These effects are mainly caused by the larger density of brine as compared to fresh water. At steady state, the pressure gradient used to overcome gravity force increases by 9.3% on average (over the entire depth) because of heavier brine (Fig. 3(b)), which directly results in less pressure gradient available for transporting the fluids (i.e. the friction and acceleration). As a result, the final total (gas+liquid) flow rate decreases by 4% from 33.1 kg/s (no salt) to 31.7 kg/s (brine). Furthermore, such decrease in total flow rate (-1.39 kg/s) due to brine effects is almost evenly distributed between gas (CO_2-rich) phase (−0.68 kg/s, 49% of the total) and liquid (water-rich) phase (−0.71 kg/s, 51% of the total). However, given the larger flow rate of liquid phase, the relative decreases are significantly different between two phases. While the liquid (water-rich) phase flow rate only decreases by 2% from 30.8 kg/s (no salt) to 30.1 kg/s (brine), the gas (CO_2-rich) phase flow rate decreases as much as 29% from 2.33 kg/s (no salt) to 1.65 kg/s (brine). Including with the effect of less dissolved CO_2 transported because of less water transport in liquid phase (less total liquid flow rate plus 3.61 kg/s of salt), the final CO_2 leakage rate decreases by 30% because of brine effects. The larger viscosity of brine, associated with larger density, also plays a role through its influences on the drift velocity (phase friction) and the friction to wall, though a smaller one. It is interesting to notice that, in a system with fixed pressures at top and bottom boundary, the total pressure drop (gradient) increases in the lower portion of the wellbore due to heavier brine but decreases in the upper portion due to smaller velocity associated with brine when the friction pressure drop (gradient) overpasses the gravity pressure drop (Fig. 3(b)).

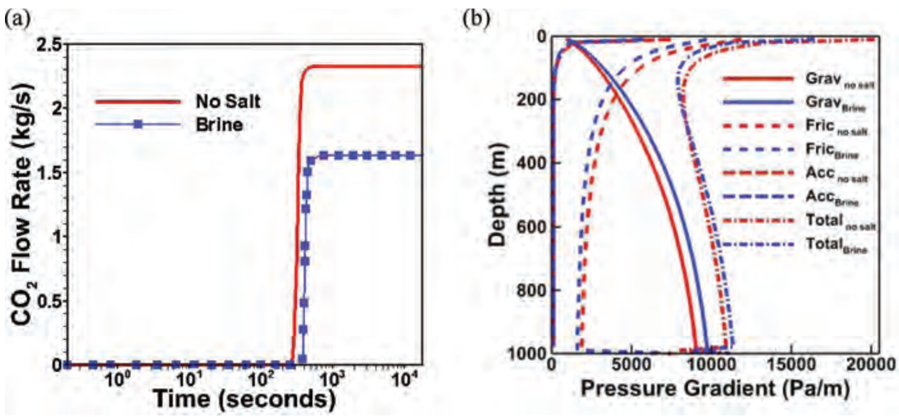

Figure 3. Case 1: The effect of brine on CO_2 (component) leakage rate through the wellhead (a) and the pressure gradients along the wellbore at 36000 s (b). Mass fraction of salt in the brine is 0.12.

Case 2. CO_2 leakage up a wellbore from a finite reservoir

In Case 1, we focused on the wellbore flow behavior and assumed that the reservoir is able to maintain constant pressure, temperature, and gas saturation throughout the leakage process. In the real world, the reservoir will not be able to maintain the constant bottom-hole conditions because of dynamic flow and depletion processes in the reservoir. The coupling between wellbore (open conduit) processes and flow in the reservoir (porous medium) is critical in controlling the leakage dynamics. In this example, we coupled a 2 km × 2 km (finite) reservoir of 10 m thickness to the same wellbore as modeled in Case 1. The wellbore is assumed to fully penetrate the reservoir and is perforated across the entire reservoir thickness. The reservoir is assumed to be radially symmetric and is represented by 13 grid cells with varied size (from 0.08 m near the wellbore to a few hundred meters in the far field). The reservoir is finite and its top, bottom, and side boundaries are closed but there is heat exchange through its bottom boundary. The major properties of the reservoir formation are presented in Table 2 (wellbore properties are shown in Table 1). The initial conditions in the wellbore and the reservoir (i.e. the bottom boundary conditions in Table 1) are the same as those in Case 1.

The simulated CO_2 flow rates at three different locations in the wellbore for Case 2 and associated pressures and gas saturations in the wellbore and in the reservoir are depicted in Fig. 4. Comparing the curves in Figs 4(a) and 1(c), the effects of reservoir processes on CO_2 leakage are apparent. In Case 2, the CO_2 flow at the wellbore bottom occurs much later and at a lower rate (Fig. 4(a)) than in Case 1 (Fig. 1(c)).

Table 2. Properties of the finite reservoir coupled to the wellbore.

Parameter	Value	Note
Permeability	10^{-12} m^2	uniform and isotropic
Porosity	0.20	uniform
Thermal conductivity	2.51 W m^{-1} K^{-1}	
Parameters for relative permeability:		Liquid relative permeability using van Genuchten-Mualem model van Genuchten, 1980) and gas relative permeability using Corey model (Corey, 1954)
Residual gas saturation	0.04	
m_{VG}	0.20	
Residual liquid saturation	0.27	
Saturated liquid saturation	1.0	
Parameters for capillary pressure:		Capillary pressure using van Genuchten model
Residual liquid saturation	0.25	
m_{VG}	0.20	
α_{VG}	0.00084 Pa^{-1}	
Maximum capillary pressure	10^5 Pa	
Saturated liquid saturation	1.0	
Pore compressibility	10^{-10} Pa^{-1}	

After the first peak associated with commencement of gas flow out of the wellhead, the CO_2 leakage rate quickly decreases to a somewhat 'stable' rate about 1.0 kg/s (Fig. 4(a)), which is much smaller than that (2.33 kg/s) in Case 1. Furthermore, the leakage rate decreases slowly but steadily over the long term (Fig. 4(a)). Within 10 days, the stable leakage rate drops from about 1.5 kg/s to less than 1 kg/s. This is mainly because of the pressure drop in the nearby formation (Fig. 4(b)) as a result of depletion due to leakage. Note that the system is still in the process of propagation of the pressure drop towards the far field boundary of the reservoir after 10 days of leakage and the far field of the reservoir has not yet 'felt' such pressure drop (Fig. 4(b)). In other words, the intrinsic reservoir properties (e.g. pressure gradient, mobility of each phase) alone can make a large difference in leakage given the same wellbore even if the finite nature of the reservoir is still not felt.

The sudden drop of the pressure at the well bottom is caused by the breakthrough of the gas bubble at the wellhead when the entire wellbore becomes a gas-filled column (Fig. 4(c)). As shown in Fig. 4(d), the time it takes to fill the upper half of the wellbore with gas phase is much shorter than that for the lower half, which is evidence of the self-acceleration (gas-lifting) process taking place. As the gas occupies more and more space, the pressure gradient needed to overcome the gravity body force becomes less and less. Rapid sweep of water from the entire wellbore occurs around 4800 s (Fig. 4(d)). Simultaneously, the high pressure gas phase breaks through at the wellhead, and subsequently pressures in the wellbore drop quickly. The peak of the leakage rate (Fig. 4(a)) reflects such a burst effect of the high pressure gas 'bubble'. From this time forward, the wellbore (more specifically the water in the wellbore) is no longer a dominant barrier for the CO_2 leakage because of very high gas saturation thorough the entire wellbore. The evolution of CO_2 leakage will depend on the pressure gradient, the formation transmissivity, on geometry, composition, and size of the CO_2 plume, and on the

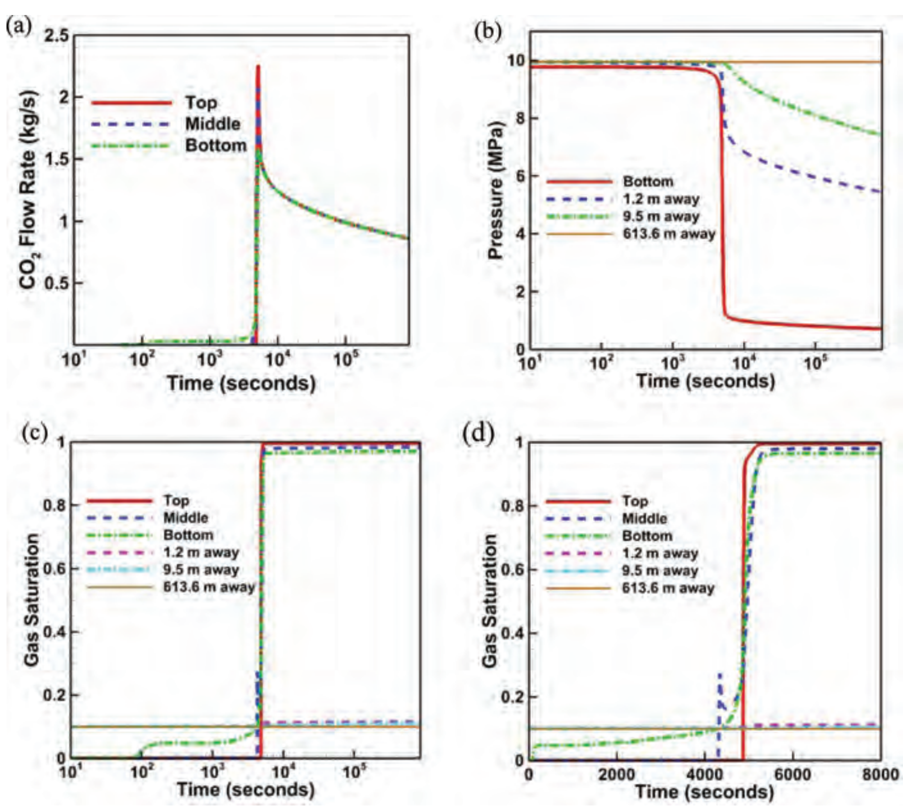

Figure 4. CO_2 (component) flow rates at three different locations for Case 2 (a) and corresponding pressure (b) and gas saturation (c) in the wellbore and reservoir. (d) is the gas saturation during the first 8000 s (linear scale).

  | *Greenhouse Gas Sci Technol.* **1**:335–350 (2011); DOI: 10.1002/ghg

leaking wellbore(s) configurations. The leakage process would likely be transient rather than steady-state. This is fundamentally different from a scenario in which bottom-hole conditions are maintained constant and the mobility of CO_2 in the reservoir would not be a limiting factor. We note that analogous flow from an oil well blowout has been observed and modeled within the last year.[27,28]

It is interesting to note that gas saturations near the wellbore (e.g. 1.2 m and 9.5 m away from the well in Figs 4(c) and 4(d)) increase in response to the pressure drop during leakage. This effect could increase the mobility of the gas-phase CO_2 in the reservoir but it is overwhelmingly compensated by the decrease of the pressure gradient in this case, resulting in a decreasing leakage rate through wellbore. The mobility of CO_2 in the reservoir is one of the critical factors controlling the leakage process through an open wellbore from reservoir. A natural question is whether a CO_2 plume with lower gas saturation in the reservoir would behave differently. To investigate this scenario, we reduced the initial gas saturation in the reservoir to 0.05 (just above the residual gas saturation 0.04 as shown in Table 2) and kept all other parameters the same as in Case 2.

The results for this reduced gas saturation scenario (Case 2-low S_g) are depicted in Fig. 5. Instead of maintaining a continuous leakage rate, reducing the initial reservoir gas saturation makes the system behave as a geyser (Fig. 5(a)). There are 39 leakage events within a 10-day period, with an average magnitude of about 0.2 kg/s, which is much smaller than the continuous leakage rate of Case 2 (Fig. 4(a)).

The detailed structure of a typical CO_2 leakage event as well as the associated gas and liquid flow rates are shown in Figs 5(b)–5(d). As shown in Fig. 5(b), the Case 2-low S_g, a leakage event begins with a sudden eruption with strongest intensity and then the flow rate gradually reduces to near zero. The leakage pattern in terms of gas phase mass flow rate (Fig. 5(d)) nearly mimics the pattern in terms of CO_2 flow rate (Fig. 5(b)), except that the gas phase mass flow rate decreases from bottom to top whereas the CO_2 flow rates are almost the same at three depths during the

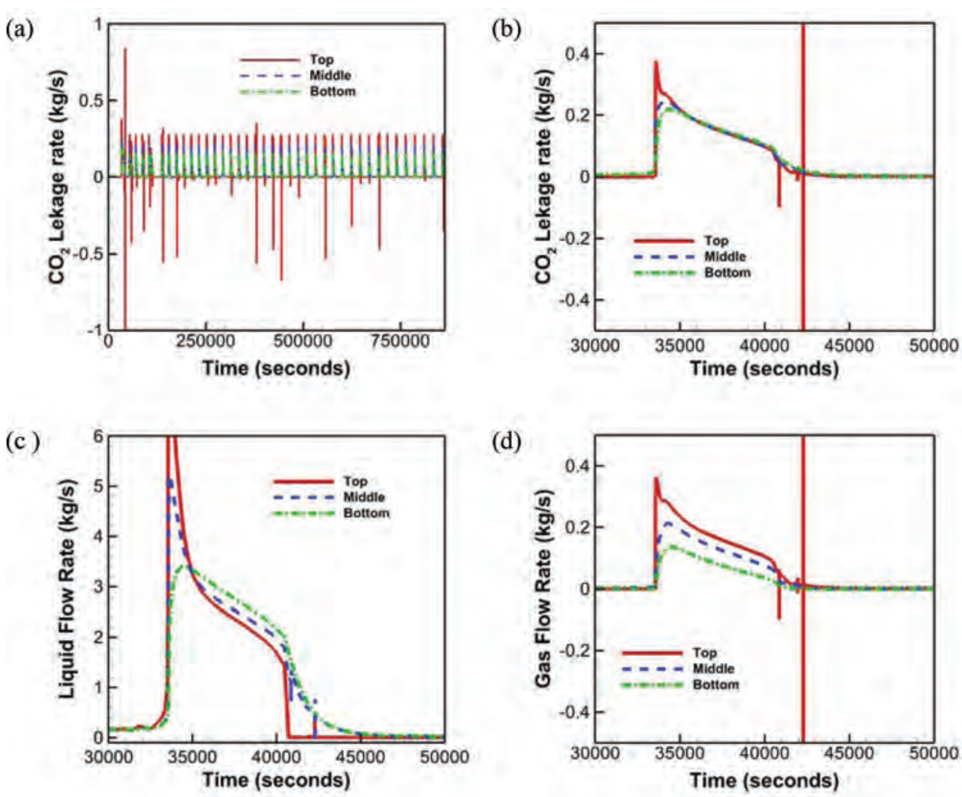

Figure 5. Simulated CO_2 flow rate at three different locations in the wellbore for an initial reservoir gas saturation of 0.05 (a) and the detailed structure of leakage events in terms of CO_2 flow rate (b), liquid flow rate (c), and gas flow rate (d).

period during which flow gradually declines. This spatial gap in CO_2 flow rate seems to be matched by the liquid phase mass flow rate (Fig. 5(c)). It is worth noting that in this two-phase flow system, the liquid flow stops at the wellhead (top) first (which causes the first negative CO_2 flow rate) and then at middle point (Fig. 5(c)). Looking closely, the liquid flow rate at the middle point (the blue dashed line in Fig. 5(c)) shows oscillations and even gets into negative territory (downward flow) at those turning points, which are responsible for the sharp oscillations of CO_2 flow at the wellhead. We note that T2Well/ECO2N does not model an air component, which means that backflow in the current model sends CO_2 down the well rather than air as would happen in reality.

The decrease in liquid phase flow towards the top (Fig. 5(c)) indicates that the well is gradually refilling with water (i.e. gas saturation decreases). As a result, the relative volume of the gas phase in the entire well decreases so that the gravity induced pressure exerted on the well bottom increases, which in turn reduces the inflow from the reservoir. In particular, such pressure increase could reduce the gas saturation in the vicinity of the well below the residual gas saturation (Fig. 6(b)) which effectively stops the gas phase flow from the reservoir to the well. Therefore, there will be no gas phase inflow until the next pressure reduction in the wellbore. As shown in Fig. 6(c), except for the first eruption, changes in gas phase flow always occur from the top downwards. In other words, the pressure decrease in the well is caused by the CO_2 exsolution under lower pressure when CO_2 saturated water flows up and reaches the wellhead. Such a pressure-relief process propagates downward very rapidly because of positive feedback provided by the gas exsolution process. The resulting bottom-hole pressure decline causes significant gas-phase inflow from the reservoir (Fig. 6(a)). However, the induced

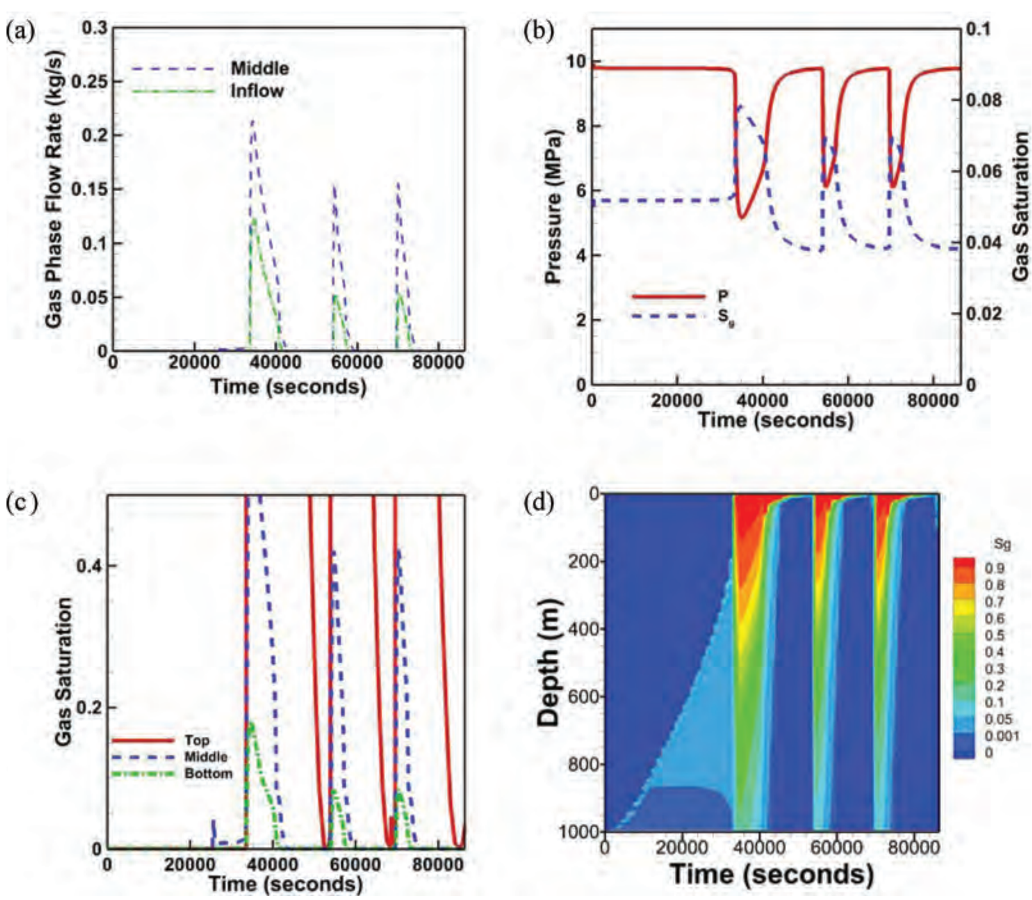

Figure 6. (a) gas phase flow into the well bottom, (b) corresponding pressure and gas saturations in the vicinity of the well in the reservoir, (c) gas saturations at three different elevations in the wellbore, and (d) gas saturation profiles in the wellbore.

  | *Greenhouse Gas Sci Technol.* **1**:335–350 (2011); DOI: 10.1002/ghg

gas phase inflow rate is not big enough to support the gas phase flow rate in the well (Fig. 5(d)). Consequently, the gas phase in the well gradually diminishes and the pressure in the well increases. Another self-reinforcing but opposite process operates until the entire wellbore is occupied by a single-phase CO_2-containing liquid.

Figure 6(d) shows a more complete picture of the transient changes in terms of the temporal evolution of gas saturation profiles in the well. At first, because the initial gas saturation in the reservoir ($S_{g0} = 0.05$) is slightly higher than the residual gas saturation ($S_{gr} = 0.04$), there is some gas phase inflow from the reservoir so that gas phase evolves at the bottom at first and then expands upward. However, because of the slight increase of pressure in the well caused by the invasion of heavier CO_2 containing water, the gas saturation near the well bottom is actually lower than that at earlier time, indicating that the bottom-hole pressure has slightly increased. In other words, the effect of heavier CO_2 containing water suppresses the gas lift effect, although not enough to hinder the inflow from the reservoir under the given conditions. However, although the earlier development of gas phase at depth is not strong enough to cause an eruption, it is responsible for the first eruption being larger and longer than the other eruption events later on because it creates a condition in which more CO_2 is stored in the well before the eruption. For each eruption cycle thereafter, the pressure reaches the maximum value when the last gas bubble of CO_2 escapes from the well right before the next eruption. As the new water (saturated with CO_2 under higher pressure) reaches the surface, gas phase occurs at the top first and reduces the pressure for the water below (i.e. creates exsolution conditions there). With the rapid propagation downward of the exsolution process, another eruption takes place until it uses up the CO_2 that can be released in gas phase in the well. Here the key point is that the gas phase inflow, as controlled by reservoir transmissivity, is not enough to support the continued gas phase flow in the well (Fig. 6(c)). Consequently, gas phase evolves from the top downward by exsolution (Fig. 6(d)). This is fundamentally different from the situation in Case 2 where the gas phase occurs at the bottom first and finally breaks through the water barrier in the well (Fig. 4(d)). In Case 2, the exsolution process only plays the role of accelerating the breakthrough process of the gas phase. The continued gas inflow from the reservoir is critical to establishing continued leakage flow through the wellbore in Case 2.

In short, the initial gas saturation in the reservoir affects not only the magnitude of the leakage flow through an open wellbore but also the dynamic pattern of the leakage in the well-reservoir system investigated above.

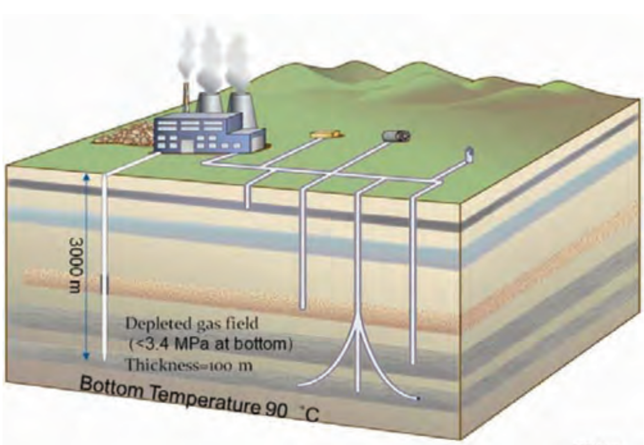

Figure 7. Sketch of injection into a depleted gas field (Case 3).

Case 3. Injection of CO_2 into a depleted gas field

This problem examines injection of CO_2 into a depleted gas field at a depth of 3000 m below the surface. The focus here is to investigate if the lower pressure in the reservoir could limit wellbore mass flow due to potential down-hole transition to subcritical (gaseous) conditions. The reservoir is assumed to have a thickness of 100 m and an area of 1 km by 1 km. It is fully perforated by a wellbore of 0.18 m in diameter. The initial pore pressure in the reservoir is arbitrarily set at approximately 3.4 MPa. The initial temperature in the reservoir is 90 °C whereas the temperature in the wellbore gradually reduces to 35 °C as it approaches the surface. An impermeable layer with a constant temperature of 90 °C is located below the reservoir formation. The permeability of the reservoir is 10^{-13} m^2. The injection rate is 100 kg/s at a temperature of 60 °C. A 2D radially symmetric grid with 416 cells (31 well cells) is used. Note the emphasis in this example is on the evolution of pressure and temperature and that compositional effects involving natural gas (CH_4) are ignored.

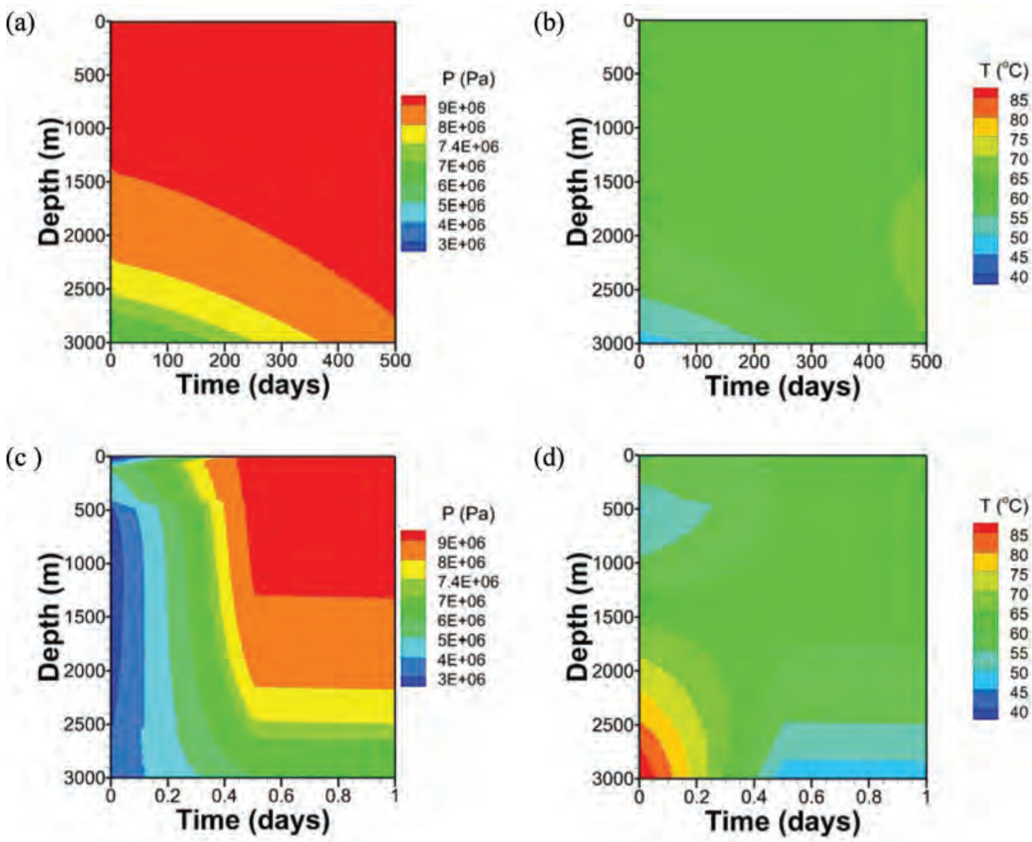

Figure 8. Case 3: Profiles of pressure and temperature in the injection wellbore as a function of time. (c) and (d) are short time (the first day) plots of (a) and (b), respectively.

As shown in Fig. 8, the lower pressure in the wellbore quickly disappears with the injection of CO_2. Within one day of injection, most of the wellbore reaches supercritical conditions (Fig. 8(c)) and the entire wellbore is in supercritical conditions after about 240 days of injection (Fig. 8(a)). The temperature profile quickly changes from geothermal gradient-dominated to convection-dominated within 1 day (Fig. 8(d)) and then becomes relatively uniform (Fig. 8(b)). The wellhead pressure quickly (within 1 day) rises above 9 MPa and remains there until the CO_2 front reaches the lateral boundary of the reservoir so that pressures in the entire reservoir rise to above the critical pressure (Fig. 9). Although the low pressure of the reservoir does keep the lower portion of the wellbore under subcritical conditions for a significant period, it does not cause a persistent limitation of mass flow rate in the wellbore. This result suggests that injection into a low-pressure reservoir is feasible and may not always require use of downhole chokes or other methods to maintain uniform CO_2 phase conditions in the well for a desired injection rate.

Discussion and conclusions

Numerical simulation of generic and idealized wellbore CO_2 leakage and injection problems suggests that coupled wellbore-reservoir flow problems are transient at early time but may reach quasi-steady states relatively quickly when changes in the reservoir conditions are not a limiting factor. For two-phase CO_2-brine leakage up a wellbore, quasi-steady-state flows are reached within minutes to hours if the reservoir can maintain a constant boundary condition at the wellbore bottom. Simulations of a more realistic wellbore-reservoir system suggest that the leakage dynamics could be much more complicated than the simple quasi-steady-state flow, especially when the two-phase inflow from the reservoir is near some threshold point. For example, the oscillation of the bottom-hole pressure due to rapid changes in

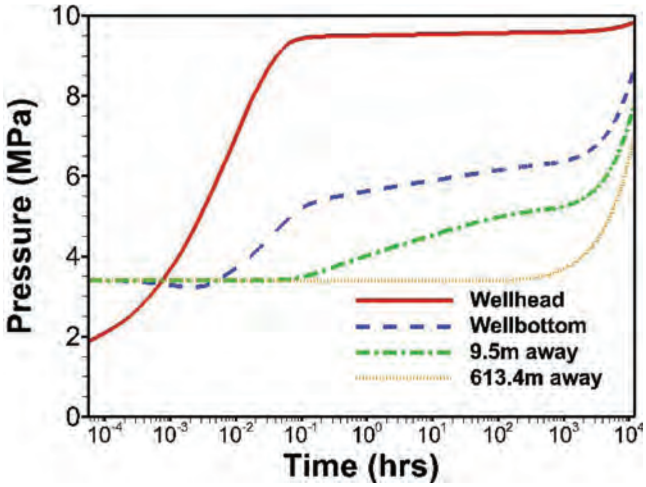

Figure 9. Case 3: Transient pressure responses to the injection at wellhead, well bottom, and two locations in the reservoir.

fluid and phase composition in the wellbore could effectively open or close off entry of gas phase from the reservoir into the wellbore. In this case, the system is not even close to any quasi-steady state. For the case of injection of CO_2 into a depleted (low-pressure) gas reservoir, overall conditions are transient for over 100 days, but the key pressure response needed to maintain single-phase conditions in the well occurs within minutes. Flow-rate limitations due to the formation of gaseous CO_2 during injection into low-pressure reservoirs are not predicted by our model.

These conclusions about the transient flow of CO_2 and brine under leakage and injection scenarios were made possible by our development and application of a non-isothermal multiphase wellbore-reservoir simulator (T2Well/ECO2N) for modeling leakage or injection of CO_2 and NaCl brine in GCS systems. The complexities of coupled reservoir-wellbore flow revealed in these examples are just a very limited sampling of scenarios that can be simulated by T2Well/ECO2N.

Appendix A. Verification

Steady-state two-phase flow upward (comparison against analytical solutions)

To verify the wellbore flow solution approach, we simulated a case of steady-state, isothermal, two-phase (CO_2 as gas and water as liquid) flow through a vertical wellbore of 1,000 m length. The details of the problem are described below (Table A1):

Table A1. Parameters of the two-phase wellbore flow problem.

Parameter	Value	Note
Length	1,000 m	Vertical wellbore
Diameter	0.1 m	Circular
Total (upward) mass flux (G)	50 kg/m^2/s	Gas + Liquid
Gas mass fraction	0.5	
Temperature	40 °C	Isothermal
Wellhead Pressure	105 Pa	

The specifications of the one-dimensional numerical solution (T2Well/ECO2N) are:

1. 1,000 m wellbore with a diameter of 0.1 m
2. Grid resolution 10 m
3. Injection mass rate at bottom: CO_2: 0.19625 kg/s; water: 0.19625 kg/s (Each = 25 kg/m2/s with a cross sectional area of 7.8500E-03 m^2)
4. Isothermal simulation with a uniform temperature of 40 °C throughout the wellbore
5. Top boundary (outlet) pressure is 10^5 Pa
6. Wall roughness 2.4e-5 m

The steady state problem is actually solved as a transient problem with adaptive time steps. The ending simulation time is 0.456869E+09 seconds (4100 steps), at which the average pressure loss due to temporal acceleration is about 3.80E-16 (Pa/m). Therefore, the steady state is considered to be reached.

As shown in Figure A1, the numerical solutions are almost identical to the analytical solutions29, thereby verifying the numerical wellbore code (T2Well/EOS3) for this particular problem. Note that the mixing between the CO_2 and the water phases is allowed in the numerical simulation but no mixing is assumed for the analytical solution. However, the almost perfect match between analytical solutions and the numerical solutions implies that the effects of the mixing between the two phases (<2%) on the two phase flow are negligible.

In this system, although the mass fraction defined as the ratio of CO_2 flow rate to H_2O flow rate is constant (X = 0.5) throughout the wellbore, the gas (CO_2-rich

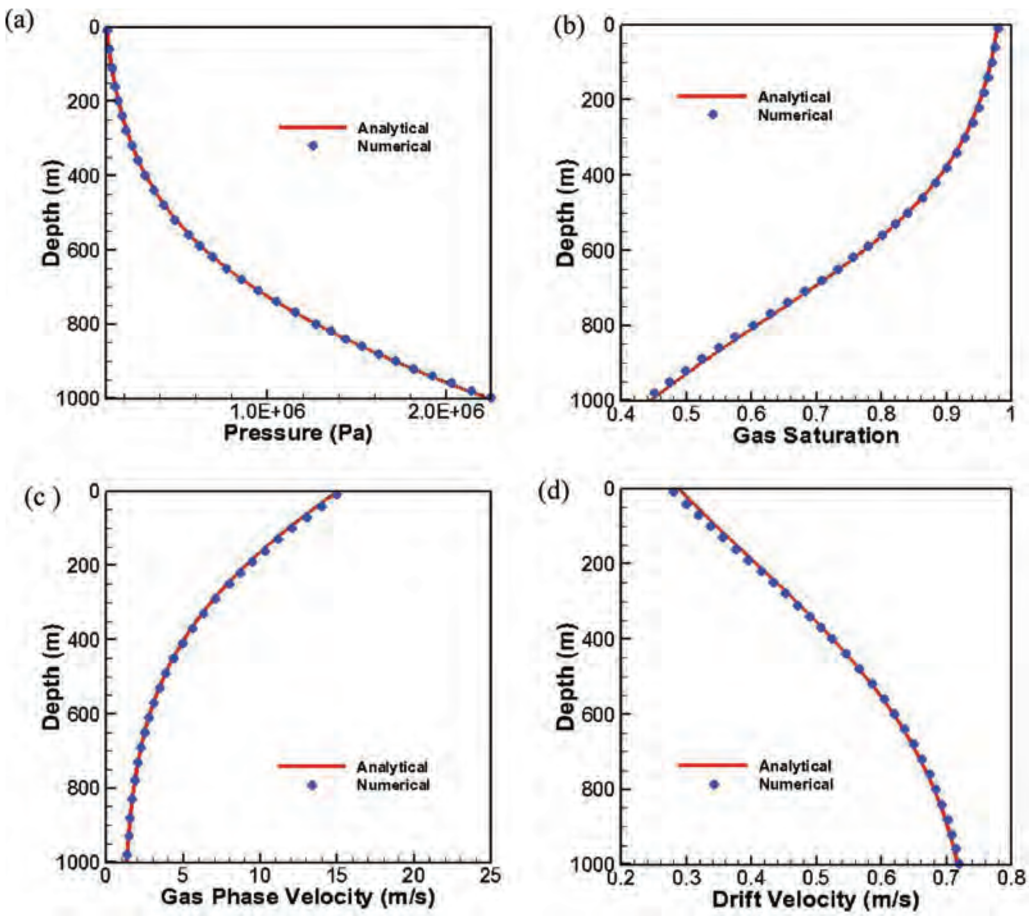

Figure A1. Distribution of pressure, gas saturation, gas-phase velocity, and drift velocity under steady-state, isothermal, two-phase (CO_2/water) flow conditions in a vertical wellbore showing excellent agreement between the two approaches.

phase) saturation decreases with depth due to pressure increase because of the low density of gas phase at the given pressure range (Figure A1). Meanwhile, the drift velocity (of the gas-phase velocity relative to the mean volumetric velocity) increases with depth from about 0.28 m/s to 0.72 m/s. However, the gas-phase velocity decreases with depth by about 11 times over 1000 meters (Figure A1).

Acknowledgements

The authors would like to thank Christine A. Doughty at LBNL for a review and many helpful suggestions and Stephen W. Webb (Sandia National Laboratories) for fruitful discussions about the drift-flux model that has been implemented in T2Well code. This work was supported, in part, by the CO_2 Capture Project (CCP) of the Joint Industry Program (JIP), by the National Risk Assessment Partnership (NRAP) through the Assistant Secretary for Fossil Energy, Office of Sequestration, Hydrogen, and Clean Coal Fuels, through the National Energy Technology Laboratory, and by Lawrence Berkeley National Laboratory under US Department of Energy Contract No. DE-AC02-05CH11231.

References

1. Apps JA, Zheng L, Zhang Y, Xu T and Birkholzer JT, Evaluation of potential changes in groundwater quality in response to CO_2 leakage from deep geologic storage. *Transport Porous Med* **82:**215–246 (2010).
2. Carey JW, Wigand M, Chipera SJ, Gabriel GW, Pawar R, Lichtner PC, Wehner SC, Raines MA and Guthrie GD, Analysis and performance of oil well cement with 30 years of CO_2 exposure from the SACROC Unit, West Texas, USA. *Int. J. Greenhouse Gas Cont* **1**(1):75–85 (2007).

3. Gasda SE, Bachu S and Celia MA, The potential for CO_2 leakage from storage sites in geological media: Analysis of well distribution in mature sedimentary basins. *Environ Geol* **46**(6/7):707–720 (2004).
4. Jordan PD and Benson SM, Well blowout rates and consequences in California oil and gas district 4 from 1991 to 2005: Implications for geological storage of carbon dioxide. *Environ Geol* **57**(5):1103–1123 (2009).
5. Ringrose P, Atbi M, Mason D, Espinassous M, Myhrer Ø, Iding M, Mathieson A and Wright I, Plume development around well KB-502 at the In Salah CO_2 storage site. *First Break* **27**(January):85–89(2009).
6. Baklid A, Korbol R and Owren G, *Sleipner vest CO_2 disposal, CO_2 injection into a shallow underground aquifer,* SPE Annual Technical Conference and Exhibition, October 6–9, 1996, Denver, Colorado, SPE-36600-MS.
7. Lindeberg E, Modelling pressure and temperature profile in a CO_2 injection well. *Energy Procedia* **4**:3935–3941 (2011).
8. Lu M and Connell LD. Non-isothermal flow of carbon dioxide in injection wells during geological storage. *Int J Greenhouse Gas Cont* **2**(2):248–258 (2008).
9. Remoroza AI, Moghtaderi B and Doroodchi E, Coupled wellbore and 3D reservoir simulation of a CO_2 EGS, *Proceedings, SGP-TR-191, 36th Workshop on Geothermal Reservoir Engineering*, Stanford University, Stanford, California, January 31–February 2, 2011
10. Livescu S, Durlofsky LJ, Aziz K, and Ginestra JC, A fully-coupled thermal multiphase wellbore flow model for use in reservoir simulation. *J Petrol Sci Eng* DOI:10.1016/j.petrol.2009.11.022 (2009).
11. Shi H, Holmes JA, Durlofsky LJ, Aziz K, Diaz LR, Alkaya B and Oddie G, Drift-flux modeling of two-phase flow in wellbores. *Soc Pet Eng J* **10**(1):24–33 (2005).
12. Zuber N and Findlay JA, Average volumetric concentration in two-phase flow systems. *J Heat Trans-T ASME* **87**(4):453–468 (1965).
13. Pruess K, *ECO2N: A TOUGH2 Fluid Property Module for Mixtures of Water, NaCl, and CO_2*, Research Report LBNL-57952. Lawrence Berkeley National Laboratory, Berkeley, CA (2005).
14. Pruess K and Spycher N, ECO2N – A fluid property module for the TOUGH2 code for studies of CO_2 storage in saline formations. *Energ Convers Manage* **48**:1761–1767 (2007).
15. Hadgu T, Zimmerman RW and Bodvarsson GS, Coupled reservoir-wellbore simulation of geothermal reservoir behavior. *Geothermics* **24**(2):145–166 (1995).
16. Pruess K. On CO_2 fluid flow and heat transfer behavior in the subsurface, following leakage from a geologic storage reservoir. *Environ Geol* **54**(8):1677–1686 (2008).
17. Pan L, Oldenburg CM, Wu Y-S and Pruess K, *T2Well/ECO2N Version 1.0: Multiphase and Non-Isothermal Model for Coupled Wellbore-Reservoir Flow of Carbon Dioxide and Water NaCl Brine,* Report LBNL-4291E. [Online]. Lawrence Berkeley National Laboratory Report, Berkeley, CA (2011). Available at: http://esd.lbl.gov/files/research/projects/tough/documentation/T2Well_ECO2N_Manual.pdf [August 10, 2011]
18. Pan L, Oldenburg CM, Wu Y-S and Pruess K, Wellbore flow model for carbon dioxide and brine, *Energy Procedia*. [Online]. Proceedings of the GHGT9 conference, November 16-20, Washington DC. LBNL-1416E (2008). Available at: http://www.sciencedirect.com/science/article/pii/S1876610209000137 [August 10, 2011]
19. Wallis GB, *One-dimensional Two-phase Flow*. McGraw-Hill Book Company, New York (1969).
20. Oddie G, Shi H, Durlofsky LJ, Aziz K, Pfeffer B and Holmes JA, Experimental study of two and three phase flows in large diameter inclined pipes. *Int J Multiphas Flow* **29**:527–558 (2003).
21. Richter HJ, Flooding in tubes and annuli. *Int J Multiphas Flow* **7**(6):647–658 (1981).
22. Pruess K, Oldenburg CM and Moridis GJ, *TOUGH2 User's Guide Version 2*, *Report LBNL-43134.* E. O. Lawrence Berkeley National Laboratory, Berkeley, CA (1999).
23. Pruess K, Integrated modeling of CO_2 storage and leakage scenarios including transitions between super- and sub-critical conditions, and phase change between liquid and gaseous CO_2. Greenhouse Gas. Sci. Tech (2011) in press.
24. Ramey HJ Jr, Wellbore heat transmission. *J Petrol Technol* **225**:427–435 (1962).
25. van Genuchten MTh, A closed-form equation for predicting the hydraulic conductivity of unsaturated soils. *Soil Sci Soc* **44**:892–898 (1980).
26. Corey AT, The interrelation between gas and oil relative permeabilities. *Producers Monthly* **November:**38–41 (1954).
27. Hsieh PA, Application of MODFLOW for oil reservoir simulation during the deepwater horizon crisis. *Ground Water* **49**(3):319–323 (2011).
28. Oldenburg CM, Freifeld BM, Pruess K, Pan L, Finsterle S and Moridis GJ, Numerical simulations of the Macondo well blowout reveal strong control of oil flow by reservoir permeability and exsolution of gas. P National Acad Sci DOI:10.1073/pnas.1105165108 (2011).
29. Pan L, Webb SW and Oldenburg CM, An analytical solution for steady-state compressible two-phase flow in a wellbore. *Adv Water Resour* (2011) in press.

Lehua Pan

Lehua Pan is a Senior Scientific Engineering Associate at Lawrence Berkeley National Laboratory, which he joined in 1997. He received his PhD in Soil Physics/Hydrology (1995), an MSc in Soil Physics (1986), and BSc in Geology (1982). He is an expert in computer modeling of Earth systems and processes.

Curtis M. Oldenburg

Curt Oldenburg is the Co-Editor-in-Chief of *Greenhouse Gases: Science and Technology.*

Yu-Shu Wu

Yu-Shu Wu is a professor and CMG Reservoir Modeling Chair at Colorado School of Mines with research interest in quantitative approaches and studies in reservoir engineering. He is also a guest scientist at Lawrence Berkeley National Laboratory (LBNL). He had BSc (Eqv.)/MSc degrees from China and MSc and PhD degrees in reservoir engineering from UC Berkeley.

Karsten Pruess

Karsten Pruess is a Senior Scientist at Lawrence Berkeley National Laboratory, which he joined in 1977. He holds a D.Phil. Nat. in physics from the University of Frankfurt (1972). He has published over 140 papers and is the chief developer of the TOUGH codes. Pruess is a member of SPE, GRC, and a Fellow of AGU and GSA, and a member of NAE (2011).

  | *Greenhouse Gas Sci Technol.* **1**:335–350 (2011); DOI: 10.1002/ghg